

## Exergy and energy analysis of solar absorption cooling system in hot regions with NH<sub>3</sub>-H<sub>2</sub>O and NH<sub>3</sub>-LiNO<sub>3</sub> refrigerant solutions

Chougui Mohamed Lamine<sup>1,2</sup> and Zid Said<sup>1</sup>

<sup>1</sup>Génie climatique, University of Constantine1, Génie climatique, Laboratory of génie climatique, Constantine, Constantine, Algeria

<sup>2</sup>Architecture, University of Jijel, science and technology, Jijel, Jijel, Algeria

Copyright © 2020 ISSR Journals. This is an open access article distributed under the *Creative Commons Attribution License*, which permits unrestricted use, distribution, and reproduction in any medium, provided the original work is properly cited.

**ABSTRACT:** In hot regions like the southern Algeria, a huge amount of energy is used for cooling. This study presents a methodology of exergy and energy analysis for ammonia-water and ammonia-lithium nitrate absorption cooling coupled to a double glazed flat plate collector. The thermal energy is stored in an insulated thermal storage tank. To compare total exergy loss and improve the coefficient of performance and exergetic efficiency for both solutions, the effects of heat exchanger efficiency, storage temperature, absorber, and condenser and evaporator temperature have been discussed in this study. Thermodynamic models have been developed using the first and second laws of thermodynamics. These models are employed in a computer program using FORTRAN to perform the calculations. Results indicate that ammonia-lithium nitrate cycles gives or even better performance than the ammonia-water cycle, Therefore, it's suitable alternative to the ammonia-water cycle. Exergy analysis shows also that the total exergy loss in the system depends strongly on the working temperatures.

**KEYWORDS:** Simulation, Performance, Optimization, Entropy, Enthalpy, Refrigeration.

### 1 INTRODUCTION

Cooling represents a significant proportion of the overall demand for energy [1]. Approximately 80% of the world's electricity is being generated from fossil fuels that contribute significantly to depletion of ozone layer and greenhouse gas emissions [2].

Although the environmental constraints imposed for limitation of the use of CFC and HCFC refrigerants have contributed to the emergence of systems using heat energy as a primary source such as sorption systems.

Furthermore, the intensive use of mechanical compression refrigeration systems is responsible for a strong peak in electricity consumption in summer, which can lead to network overloads [3],

Another concern with conventional cooling is the availability of energy; indeed, in rural areas where the conventional electricity network is lacking, cooling is a serious problem.

That makes solar cooling technology a suitable alternative who could reduce energy needs during the peak periods in summer by replacing electrically driven compressor chillers with thermally driven chillers; especially in hot regions (the Middle East and North Africa).

The most common method for producing thermally activated cooling is sorption cooling. Sorption includes both absorption and adsorption, but the solar thermal with single-effect absorption system with the mature technology come into view to be the best option [4].

Recently, more than 50 solar-powered cooling projects through Europe in different climatic zones were surveyed and analysed to identify future needs and evaluate the overall prospects of solar cooling [5]

Several researchers presented recently modelling and simulation studies of solar cooling systems. Divers numerical models for describing the performance characteristics of absorption chillers are presented in [6], [7], [8]. The exergy and energy analysis of absorption cooling systems without solar collector is made by several authors [9], [10]. S.C. Kaushik and al [11] present the exergy analysis and the effects of generator, absorber and evaporator temperatures on the energy and exergy performances of the single effect water–lithium bromide absorption system without solar collector.

Sencan and al [12] investigated exergy analysis of a single-effect LiBr–H<sub>2</sub>O absorption system; they evaluated the coefficient of performance, exergetic efficiency and exergy loss in each component of the system

Dehua Cai and al [13] consider that NH<sub>3</sub>/LiNO<sub>3</sub> absorption refrigeration cycles is considered to be the most possible ones for application in small capacity refrigeration units. Also, NH<sub>3</sub>/LiNO<sub>3</sub> absorption refrigeration systems can provide cooling capacity at evaporating temperature of  $T_e < 0$ , which cannot be obtained by the H<sub>2</sub>O–LiBr systems, and, NH<sub>3</sub>/LiNO<sub>3</sub> systems do not need a rectifier for refrigerant purification when comparing to the NH<sub>3</sub>–H<sub>2</sub>O systems.

Tyagi [14] presented a second law based thermodynamic study of NH<sub>3</sub>/NaSCN absorption refrigeration cycle and the analysis result was compared to the vapor compression cycle's, however, Tyagi did not provide a methodology to obtain thermophysical properties especially the entropy value of the NH<sub>3</sub>/NaSCN solution. Zhu and Gu [15] theoretically studied NH<sub>3</sub>/NaSCN absorption refrigeration cycle using both the first and second law of thermodynamics.

In order to improve the performance of a solar absorption refrigeration system, many optimization studies based on exergy and energy analysis have been done.

Ravikumar and al [16] study the influence of both generators temperatures of a double-effect solar absorption system on exergy values.

Ghaddar and al [17] modeled and simulated a solar absorption system for a typical house in Beirut.

However, in Mazloumi et al work [18] a solar single effect lithium bromide–water absorption cooling powered by a horizontal N–S parabolic trough collector has simulated.

Talbi and al [19] studied the exergy analysis of an absorption refrigeration system using H<sub>2</sub>O–LiBr.

In Onan et al paper [20], the hourly exergy destruction for each component in solar absorption cooling system is analyzed.

The performance of solar absorption cooling system under different operating is shows by Fellaah and al [21] in order to find the optimum conditions for which the maximum refrigeration effect can be achieved.

In the present paper, we carry out a first and second law based thermodynamic simulation for solar absorption cooling system in the region of Adrar- Algeria- with NH<sub>3</sub>–H<sub>2</sub>O and NH<sub>3</sub>–LiNO<sub>3</sub> refrigerant solutions in order to compare total exergy loss and improve the coefficient of performance and exergetic efficiency for both solutions.

## 2 METHODOLOGY

### 2.1 DESCRIPTION AND MODELING OF SYSTEMS

Solar absorption cooling systems usually consist of solar thermal collectors linked to an absorption chiller; a storage tank is essential to ensure stable and continuous separation at the generator; auxiliary heater can also be used for the night.

The water heated by the solar collector is stored in the storage tank and pumped to the generator to separate the refrigerant from the absorbent.

The heat is provided by double glazed flat plate collector, which is capable of delivering 70 -120°C fluid to the generator. A single effect ammonia-water absorption chiller can be driven by this generator temperature at a COP of 0.3-0.7 [22].

The ammonia water cycle requires a rectifier to purify the ammonia because both water and ammonia are volatile. Without a rectifier, the ammonia vapor from the generator may contain some water vapor, which could form ice in the condenser [23].

Then, the superheated refrigerant is condensed in the condenser by the cold water of the cooling tower, water follows through the expansion valve and arrived to the evaporator to produce cold required. The vapor is lead to the absorber where it is absorbed by the rich solution coming from the generator; finally, the rich solution is pumped to the generator via a solution heat exchanger.

Fig. 1 shows the schematic diagram of the solar ammonia–water absorption cooling system.



For the absorber:

$$\frac{dM_{total\ mass}}{dt} = m_3 + m_{10} - m_4 = 0 \quad (6)$$

$$\frac{dM_{Refrigerant\ mass}}{dt} = m_{10}x_{10} - m_4x_4 = 0 \quad (7)$$

$$\frac{dU}{dt} = Q_a - m_3h_3 - m_{10}h_{10} + m_4h_4 = 0 \quad (8)$$

For the condenser:

$$\frac{dM_{total\ mass}}{dt} = m_7 - m_1 = 0 \quad (9)$$

$$\frac{dU}{dt} = Q_c - m_1(h_1 - h_7) = 0 \quad (10)$$

For the evaporator:

$$\frac{dM_{total\ mass}}{dt} = m_3 - m_2 = 0 \quad (11)$$

$$\frac{dU}{dt} = Q_e - m_2(h_3 - h_2) = 0 \quad (12)$$

For the pump:

$$\frac{dM_{total\ mass}}{dt} = m_4 - m_5 = 0 \quad (13)$$

$$\frac{dU}{dt} = \int VdP = W_p - m_4(h_5 - h_4) = 0 \quad (14)$$

For the heat exchanger:

$$\frac{dM_{total\ mass}}{dt} = m_5 - m_6 = 0 \quad (15)$$

$$\frac{dM_{total\ mass}}{dt} = m_8 - m_9 = 0 \quad (16)$$

$$\frac{dU}{dt} = m_5(h_6 - h_5) - m_8(h_8 - h_9) = 0 \quad (17)$$

The coefficient of performance (COP) is the ratio of the useful energy gained from the evaporator to the primary energy supply to the generator and mechanical work done by the pump of the system [25].

$$COP = \frac{\text{useful energy output}}{\text{primary energy input } + \text{ work done by pump}} = \frac{Q_e}{Q_g + W_p} \quad (18)$$

### 2.2.2 SECOND LAW ANALYSIS (EXERGY METHOD)

Exergy is defined as the maximum amount of work potential of a material or an energy stream, in relation to the surrounding environment [25]. In steady state and neglecting the kinetic energy and the potential energy and according to [26], the exergy balance equation applied to a fixed control volume is given by:

$$Ex_D = (\sum_i m_i e_i)_{in} - (\sum_i m_i e_i)_{out} + \sum_i Q_i \left(1 - \frac{T_0}{T_i}\right)_{in} - \sum_i Q_i \left(1 - \frac{T_0}{T_i}\right)_{out} + \sum W = 0 \quad (19)$$

Where  $Ex_D$  represents the rate of exergy loss of each component in the system. On the right hand side of the equation, the first two terms represent the amount of the exergy entering and leaving the steady flow process in terms of mass transfer. The third and fourth terms are the exergy loss in terms of heat transfer maintained at constant temperature. The last term is the mechanical work transfer to or from the control volume.

The exergy per unit mass of a fluid stream can be defined as [27]:

$$e = (h - h_0) - T_0 (S - S_0) \quad (20)$$

Where  $e$  is the specific exergy,  $h$  and  $S$  are the enthalpy and entropy of the fluid at temperature  $T$ , whereas,  $h_0$  and  $S_0$  are the enthalpy and entropy of the fluid at environmental temperature  $T_0$ . In this analysis,  $T_0$  was set to 298.15 K. The exergy loss in each component and the total exergy loss for the system can be written as:

$$Ex_{D,g} = m_6 e_6 - m_7 e_7 - m_8 e_8 + Q_g \left(1 - \frac{T_0}{T_g}\right) \quad (21)$$

$$Ex_{D,a} = m_4 e_4 - m_3 e_3 - m_{10} e_{10} - Q_a \left(1 - \frac{T_0}{T_a}\right) \quad (22)$$

$$Ex_{D,c} = m_7 (e_7 - e_1) - Q_c \left(1 - \frac{T_0}{T_c}\right) \quad (23)$$

$$Ex_{D,e} = m_2 (e_2 - e_3) + Q_e \left(1 - \frac{T_0}{T_e}\right) \quad (24)$$

$$Ex_{D,total} = \sum_i Ex_{Di} \quad (25)$$

The exergetic efficiency is defined as the ratio of the useful exergy gained from a system to that supplied to the system [28]

$$\zeta = \frac{\text{Exergie utile}}{\text{consommation goloable d'exergie}} = \frac{Q_e \left(1 - \frac{T_0}{T_e}\right)}{Q_g \left(1 - \frac{T_0}{T_g}\right) + W_p} \quad (26)$$

The equations necessary for the calculation of thermodynamic and physical properties of the binary solutions are given by works in the literature [29], [30], [31].

### 2.3 SOLAR UNIT ANALYSIS

The modeling of the double glazed flat plate collector was based on the equations presented in the literatures [32]. The rate of useful energy gain delivered by the solar collector can be defined as:

$$Q_u = A_c [I_g F_R (\tau\alpha) - F_R U_L (T_s - T_{am})] \quad (27)$$

Where  $A_c$  is the collector area,  $I_g$  is the solar intensity

### 2.4 THERMAL STORAGE TANK

In this type of installation in which a storage unit is placed in series with the solar collector, the temperature of the fluid entered  $T_{fe}$  in the collector is equal at each moment to the fluid temperature  $T_{storage}$  in the storage volume. We can make the simplifying assumption that the variation of  $T_{storage}$  between two instants  $t$  and  $t + \Delta t$  has a negligible influence on the value of the useful energy  $Q_u$ . We can then calculate the useful energy between  $t$  and  $t + \Delta t$ ;  $T_{fe}$  assuming constant and equal to  $T_{storage}(T)$ . Then we have:

$$T_{storage}(t + \Delta t) = T_{storage}(t) + \frac{Q_u \times \Delta t}{Cp_{storage}} \quad (28)$$

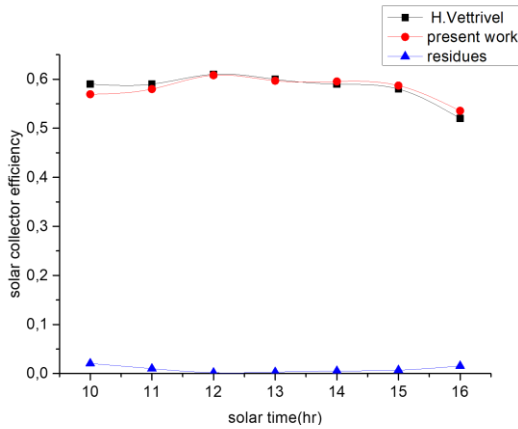


Fig. 2. Comparison of  $I_g$  values with solar time between present study and H.Vettrivel.

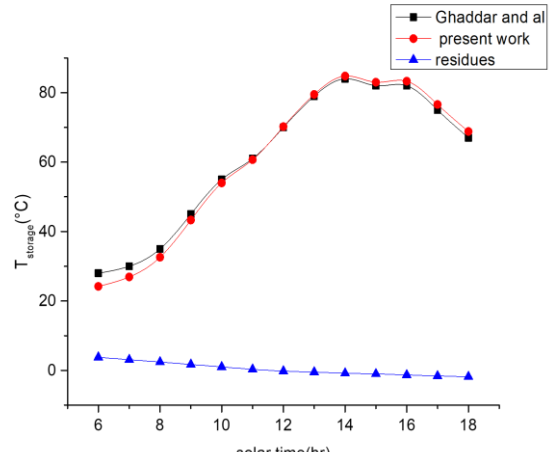


Fig. 3. Comparison of  $T_{storage}$  values with solar time between present study and ghaddar and al.

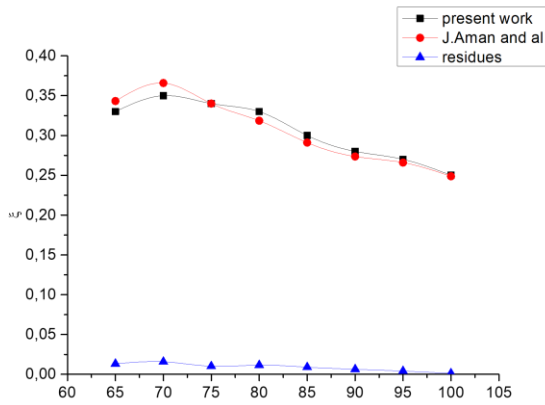


Fig. 5. Comparison of  $T_g$  values with exergetic efficiency between present study and J.Aman and al.

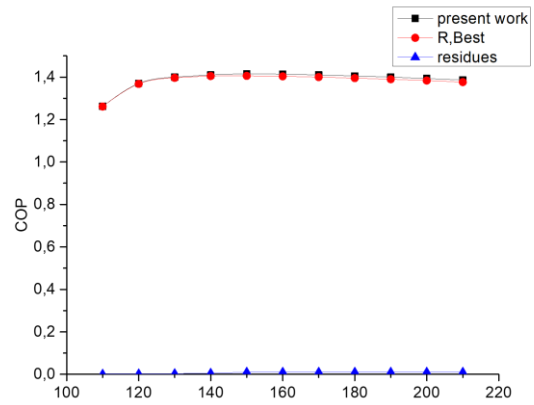


Fig. 4. Comparison of  $T_g$  values with COP between present study and R.Best.

## 2.5 MODEL VALIDATION

The computer program developed has been validated by comparing the simulation results with some available results in the literature. For the solar collector our results were compared to that of H.Vettrivel and al [33]. In their article, the authors compare the performance of a single-glazed solar collector with a double-glazed solar collector in the region of Pondicherry, India. The authors took experimental measurements between 10: 00 am and 4: 00 pm with an inclination of 12 ° and an orientation to the southeast, with  $FR (\tau\alpha) = 0.83$  and  $FR (UL)$  ranging from 3.4 to 3.8  $W/m^2C$  and  $Q_u$  values between 134 and 240 W. For the same experimental conditions we have a relatively small amplitude of the residues and an average absolute difference equal to 1.58%; fig. 2.

For the storage tank, our results have been compared with those of GHADDAR et al, [17].

In their work, the authors studied a single-effect absorption system of 10.5kW with a solar collector and a storage tank of 1m<sup>3</sup> with 3.5m<sup>3</sup> / h of volume flow rate in the city of Beirut, Lebanon.

The results had been taken between 6.15 am and 6.15 pm. The amplitude of the residues decreased compared to the evaluation of the temperature in the storage tank with an average deviation of 1.5 °C (3%) fig. 3. For absorption system, variations of COP and  $\zeta$  with generator temperatures are shown in fig. 4 and fig. 5.

Our results have been compared with those of R.Best and Aman and al. For  $T_e = -20$  °C;  $T_c = 30$  °C;  $T_a = 30$  °C in R.Best research and  $T_e = 2$  °C;  $T_c = 30$  °C;  $T_a = 30$  °C in Aman and al research. The results of present study are in good agreement

with results reached in the literature, then we can conclude that our computer program is able to predict correctly the behaviour of solar absorption cooling system.

### 3 RESULTS AND DISCUSSION

The different results presented in this work are obtained from solving the equations of the Thermodynamic models developed above. These models are employed in a computer program using FORTRAN to perform the study of the effect of various parameters on system efficiency and the performance of each component of the absorption cooling system for both NH<sub>3</sub>-H<sub>2</sub>O and NH<sub>3</sub>-LiNO<sub>3</sub>.

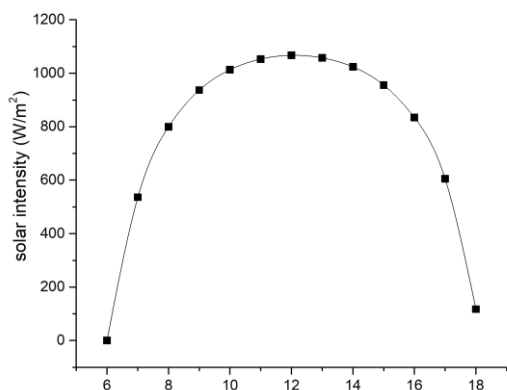


Fig. 6. Instantaneous solar radiation incident for design day of July

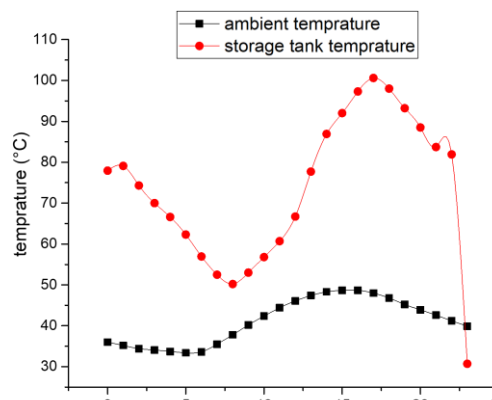


Fig. 7. Variation of ambient Temperature and storage tank temperature for design day of July

Fig. 6 shows the instantaneous solar radiation incident on a horizontal surface for the design day of July in hot city lake Adrar in Algeria; As can be noticed, the value of  $I_g$  is about 285W/m<sup>2</sup> in the morning and it arrived to 1067 W/m<sup>2</sup> at 13h. The ambient temperature and the storage tank temperature of the design day of July are shown in fig. 7. It has been assumed that the initial temperature of the storage tank and the inlet water temperature to the collector are equal to the ambient temperature.

The temperature of the storage tank varies from the temperature of 49°C to a maximum of 98°C at 15h, then it decreases to 77°C at the end of the day.

Then, temperature distribution of the storage tank can keep the absorption cooling system working well all day long.

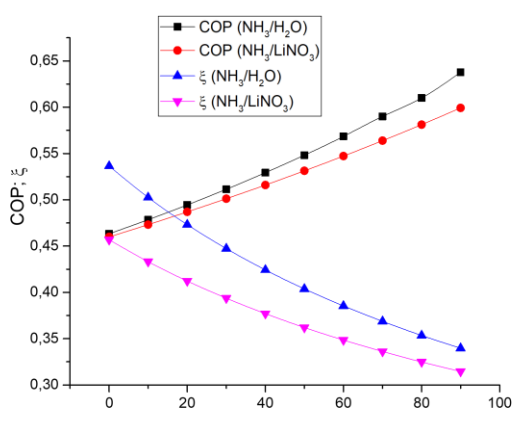


Fig. 8. Effect of Heat exchanger efficiency on (COP) and exergetic efficiency

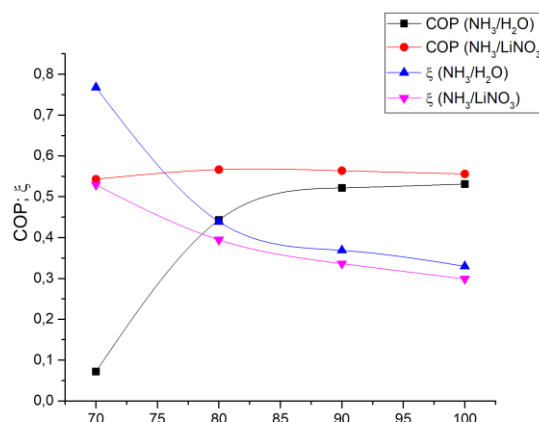


Fig. 9. Effect of storage temperature On (COP) and exergetic efficiency

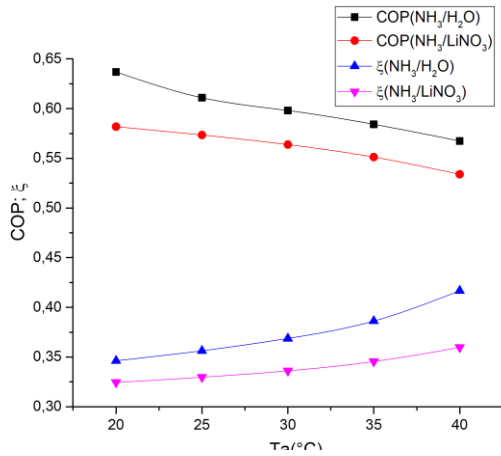


Fig. 10. Effect of absorber temperature on (COP) and exergetic efficiency

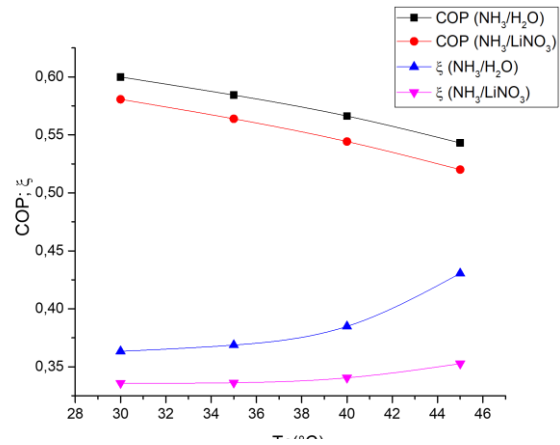


Fig. 11. Effect of condenser temperature on (COP) and exergetic efficiency

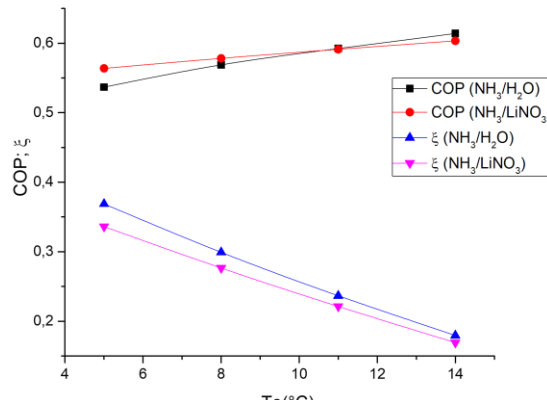


Fig. 12. Effect of evaporator temperature on (COP) and exergetic efficiency

Fig. 8 shows the comparison of coefficient of performance (COP) and exergetic efficiency ( $\zeta$ ) values as functions of effectiveness of the solution heat exchanger (Eff) for NH<sub>3</sub>-H<sub>2</sub>O, NH<sub>3</sub>-LiNO<sub>3</sub> absorption cycles.

The rise of solution heat exchanger efficiency (Eff) generates increase of coefficient of performance values, with a small advantage of (NH<sub>3</sub>/H<sub>2</sub>O).

Otherwise, exergetic efficiency is negatively affected by the rise of heat exchanger efficiency results show that low exergetic efficiency values obtained when the values of effectiveness of the solution heat exchanger (Eff) increasing for a fixed storage temperature ( $T_s$ ).

The COP values for these tow cycles increase with storage tank temperature. Fig. 9. There exists a low generator temperature limit for each cycle. Each cycle cannot be operated at generator temperatures lower than its limit. NH<sub>3</sub>-LiNO<sub>3</sub> cycle can be operated at lower generator temperature. This is an important point for utilizing solar energy since fluid temperatures for flat plate solar collectors are generally below 90°C. It is shown that, for generator temperatures less than 80°C, the NH<sub>3</sub>-LiNO<sub>3</sub> cycle gives best performance than NH<sub>3</sub>-H<sub>2</sub>O; beyond 80°C, the differences among them are not very remarkable.

The (COP) values influence the variation of exergetic efficiency ( $\zeta$ ), since ( $\zeta$ ) is equal to the product of (COP) and of a term containing the storage temperature.

As the storage temperature increases, the value of this term decreases. The exergetic efficiency ( $\zeta$ ) decreases with the increase of  $T_s$ . beyond 90 ° C, exergetic efficiency begins to stabilize.

The relationship between the (COP), exergetic efficiency and absorber temperature are shown in Fig. 10. A decrease of the system performance efficiency occur with increasing absorber temperature, on the other hand the rise of absorber temperature causes the increase of exergetic efficiency.

The result of the condenser temperature's effect is the same as that of the absorber temperature for both the system performance and for NH<sub>3</sub>-H<sub>2</sub>O and NH<sub>3</sub>-LiNO<sub>3</sub> cycles. Fig. 11

The effects of the evaporator temperature are illustrated in Fig. 12. With the increase in evaporator temperature, the (COP) values for each cycle increase however, the increase in evaporator temperature leads to the increase in (COP) and the decrease in the factor  $\left(1 - \frac{T_0}{T_e}\right) / \left(1 - \frac{T_0}{T_g}\right)$  and therefore the decrease in exergetic efficiency.

The NH<sub>3</sub>-LiNO<sub>3</sub> cycle gives best (COP) in low evaporator temperature. However, for high evaporator temperature, the performance of the NH<sub>3</sub>-H<sub>2</sub>O cycle is better than that of the NH<sub>3</sub>-LiNO<sub>3</sub> cycle.

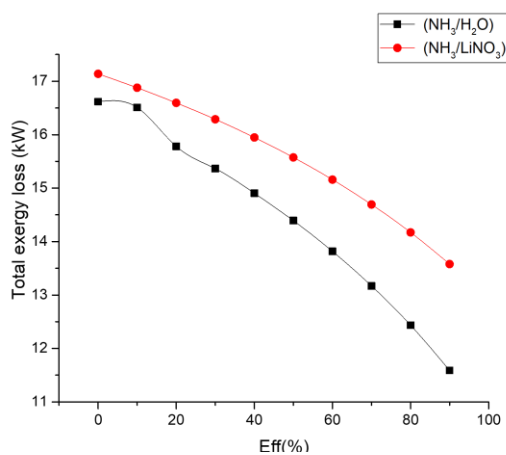


**Fig. 13. Effect of Heat exchanger efficiency on total exergetic loss**

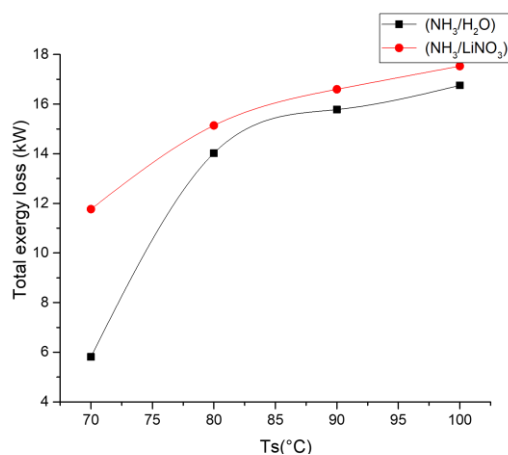


**Fig. 14. Effect of storage temperature on total exergetic loss**

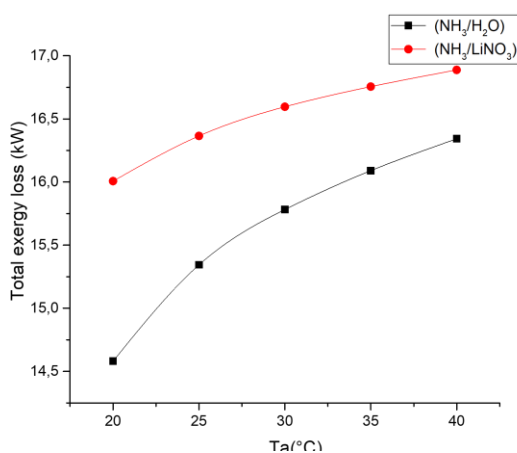


**Fig. 15. Effect of absorber temperature on total exergetic loss**

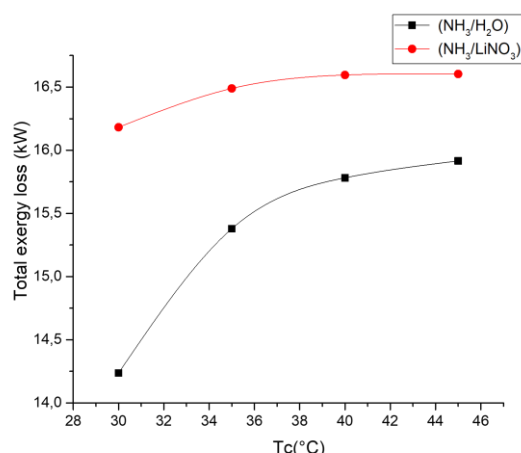


**Fig. 16. Effect of condenser temperature on total exergetic loss**

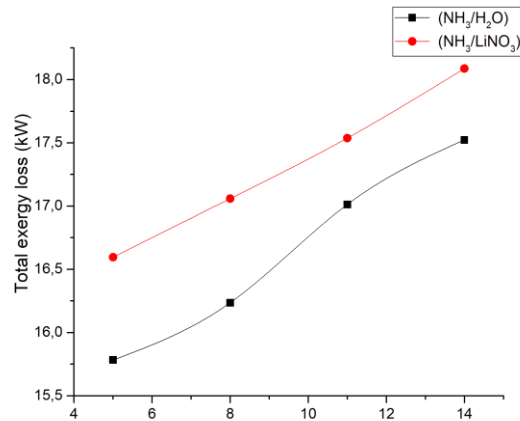


**Fig. 17 Effect of evaporator temperature on total exergetic loss**

The presence of the heat exchanger within the system substantially reduced the total exergy loss across the components, mostly in the generator and absorber. As indicated in Fig.13. Thus, increasing the effectiveness of the solution heat exchanger (Eff) improved the performance of the absorption chiller by reducing the exergy loss across the main components of the chiller.

Although, the highest generator temperature can produce more ammonia vapor, it also increases the solution temperature in the absorber and the generator, which leads to more exergy losses in the main components of the absorption system. As a result, the total exergy loss of the system is varying with the generator temperature as presented in Fig.14.

Fig. 15 illustrates the corresponding effect of the system exergy loss versus absorber temperature. Energy and exergy analyses of each component of the cooling absorption system reveals that the absorber, the generator, and the condenser represent the most of the total exergy losses of the chiller.

It can also be seen from Fig. 16 that the total exergy loss also increases rapidly with highest condenser temperature. The exergy loss in the condenser results from the temperature difference between the environment and the condenser refrigerant. So the exergy and the system performance benefit from lower condenser temperatures.

It is also shown in Fig. 17 that increasing evaporator temperature has very little impact on the total exergy loss across the components as compared to increasing the generator temperature. It can be explained that the required cooling effect can be accomplished by decreasing the evaporator temperature.

#### 4 CONCLUSION

The purpose of this study is to conduct a comprehensive analysis to compare operation of solar absorption systems in hot regions with NH<sub>3</sub>-H<sub>2</sub>O and NH<sub>3</sub>-LiNO<sub>3</sub>. Achieving this goal plays an important and vital role in encouraging and activating alternative energy investment. Based on the work described here, it is possible to make the following conclusions: The use of solar double glazed flat plate collector and insulated thermal storage tank with a single effect ammonia-lithium nitrate or ammonia-water absorption cooling system is an effective solution to hot region. The performances of these two cycles against various effectiveness of the solution heat exchanger, storage, absorber, condenser and evaporator temperatures are compared. The results show that the ammonia-lithium nitrate cycles give almost the same performances than the ammonia-water cycle. Thus, its suitable alternative to the Ammonia-water cycle. To design and optimize performance of the whole system, the most important variable is the hot source temperature while the other parameters are input variables as they are fixed by existing initial conditions.

Adopting typical values of input parameters encountered in hot regions, the system performance takes its optimal value at temperatures between 80 and 90 °C.

## **NOMENCLATURE**

A<sub>c</sub>: collector area (m<sup>2</sup>)  
C<sub>p storage</sub>: specific heat of storage water (J/kg K)  
E: specific exergy (kJ/kg)  
Eff: effectiveness of the solution heat exchanger  
E<sub>xD</sub>: exergy destruction or loss (kW)  
FR: the collector heat removal factor  
h: specific enthalpy (kJ/kg)  
h<sub>0</sub>: specific enthalpy at reference temperature 25 °C  
I<sub>g</sub>: global solar intensity (W/m<sup>2</sup>)  
m: mass flow rate (kg/sec)  
M: mass (Kg)  
p: pressure (kPa)  
P: pump  
Q: heat transfer rate (kW)  
Q<sub>u</sub>: useful energy (kW)  
S: specific entropy (kJ/kg K)  
S<sub>0</sub>: specific entropy at reference temperature 25° C  
t: time (h)  
T: temperature (K)  
T<sub>0</sub>: reference temperature 25 °C  
T<sub>fe</sub>: temperature of the fluid entered (K)  
U: the change of internal energy (kW)  
U<sub>i</sub>: the overall heat transfer coefficient (W/m<sup>2</sup> K)  
V: volume (m<sup>3</sup>/kg)  
W: work rate (kW)  
x: mass fraction of refrigerant (%)  
Δt: time period (h)

### **Subscripts**

a: absorber  
am: ambient temperature  
c: condenser  
e: evaporator  
g: generator  
i: i state point or index i = 1, 2, 3...  
s: storage

### **Greek**

ζ: exergetic efficiency  
α: absorptance  
τ: transmittance

## REFERENCES

- [1] Changements climatiques 2014: incidences, adaptation et vulnérabilité. Résumé à l'intention des décideurs, 2014.
- [2] K.F. Fong, T.T. Chow, C.K. Lee, Z. Lin, L.S. Chan, Comparative study of different solar cooling systems for buildings in subtropical city, *Solar Energy* 84 (2010) 227-244.
- [3] Papadopoulos A.M, Oxizidis S, Kyriakis N, Perspectives of solar cooling in view of the developments in the air conditioning sector, *Renewable and Sustainable Energy Reviews*, 7, 419-438, 2003.
- [4] Florides, G.A., Tassou, S.A., Kalogirou, S.A. and Wrobel, L.C. (2002) Review of Solar and Low Energy Cooling Technologies for Buildings. *Renewable and Sustainable Energy Reviews*, 6, 557-572.
- [5] Balaras, C.A., Grossman, G., Henning, H., Ferreira, C.A., Podesser, E., Wang, L. and Weimken, E. (2007) 'Solar air conditioning in Europe—an overview', *Renewable and Sustainable Energy Reviews*, Vol. 11, No. 2, pp. 299-314.
- [6] Joudi, K.A. and Lafta, A.H. (2001) 'Simulation of a simple absorption refrigeration system', *Energy Conversion and Management*, Vol. 42, No. 13, pp. 1575-1605.
- [7] Klomfar, J. and Pátek, J. (2006) 'A computationally effective formulation of the thermodynamic properties of LiBr-H<sub>2</sub>O solutions from 273 to 500K over full composition range', *International Journal of Refrigeration*, Vol. 29, No. 4, pp. 566-578.
- [8] Karamangil, M. I., Coskun, S., Kaynakli, O. and Yamankaradeniz, N. (2010) 'A simulation study of performance evaluation of single-stage absorption refrigeration system using conventional working fluids and alternatives', *Renewable and Sustainable Energy Reviews*, Vol. 14, No. 7, pp. 1969-1978.
- [9] Morosuk T, Tsatsaronis G. A new approach to the exergy analysis of absorption refrigeration machines. *Energy* 2000; 33: 890-907.
- [10] Gebreslassie, B.H., Medrano, M. and Boer, D. (2010) 'Exergy analysis of multi-effect water – LiBr absorption systems: From half to triple effect', *Renewable Energy*, Vol. 35, No. 8, pp. 1773-1782.
- [11] Kaushik, S. C. and Arora, A. (2009). *International Journal of Refrigeration*, Vol. 32, pp. 1247-1258.
- [12] Şencan, A., Yakut, K. A., & Kalogirou, S. A. Exergy analysis of lithium bromide/water absorption systems. *Renewable energy*. 2005 Apr 1; 30 (5): 645-57.
- [13] Dehua Cai, Guogeng He, Qiqi Tian, Weier Tang. (2014) 'Exergy analysis of a novel air-cooled non-adiabatic absorption refrigeration cycle with NH<sub>3</sub>-NaSCN and NH<sub>3</sub> LiNO<sub>3</sub> refrigerant solutions', *Energy Conversion and Management* 88 (2014) 66–78.
- [14] Tyagi K. Second law analysis of NH<sub>3</sub>-NaSCN absorption refrigeration cycle. *J Heat Recov Syst* 1986; 6: 73–82.
- [15] Zhu L, Gu J. Second law-based thermodynamic analysis of ammonia/sodium thiocyanate absorption system. *Renewable Energy* 2010; 35: 1940–6.
- [16] Ravikumar, T.S., Suganthi, L. and Anand A.S. (1998) Exergy Analysis of Solar Assisted Double Effect Absorption Refrigeration System. *Renewable Energy*, 14, 55-59.
- [17] Ghaddar NK, Shihab M, Bdeir F. Modeling and simulation of solar absorption system performance in Beirut. *Renew Energy* 1997; 10: 539–58.
- [18] Mazloumi M, Naghashzadegan M, Javaherdeh K. Simulation of solar lithium bromide–water absorption cooling system with parabolic trough collector. *Energy Convers Manage* 2008; 49: 2820–32.
- [19] Talbi, M.M. and Agnew, B. (2000) 'Exergy analysis: an absorption refrigerator using lithium bromide and water as the working fluids', *Applied Thermal Engineering*, Vol. 20, pp. 619-630.
- [20] Onan, C., Ozkan, D.B. and Erdem, S. (2010) Exergy Analysis of a Solar Assisted Absorption Cooling System on an Hourly Basis in Villa Applications. *Energy*, 35, 5277-5285.
- [21] Fellah A., Hamed, M. and Brahim, A.B. (2014) On the Performance of a Solar Driven Absorption Refrigerator. *Energy and Power Engineering*, 6, 278-291.
- [22] R.Z. Wang, T.S. Ge, C.J. Chen, Q. Ma, Z.Q. Xiong, Solar sorption cooling systems for residential applications: options and guidelines, *Int. J. Refrig.* 32 (2009) 638-660.
- [23] S. Raghuvansh, G. Maheshwari, Analysis of ammonia/water (NH<sub>3</sub>-H<sub>2</sub>O) vapour absorption refrigeration system based on first law of thermodynamics, *Int. J. Sci. Eng. Res.* 2 (2011) 2229-5518.
- [24] Krüger D, Pitz-Paal R, Lokurlu A, Richarts F. Solar cooling and heating with parabolic trough collectors for a hotel in the mediterranean Proceedings of the 11th SOLARPACES international symposium on concentrated solar power and chemical energy technologies, September 4-6, Zurci, Switzerland 2002 p. 83-9.
- [25] A.I. Shahata, M.M. Aboelazm, A.F. Elsafty, Energy and exergy analysis for single and parallel flow double effect water-lithium bromide vapor absorption systems, *Int. J. Sci. Technol.* 2 (2012) 85-94.
- [26] Sencan, K.A. Yakuta, S.A. Kalogirou, Exergy analysis of lithium bromide/ water absorption systems, *Renew. Energy* (2005) 645-657.

- [27] A.I. Shahata, M.M. Aboelazm, A.F. Elsafty, Energy and exergy analysis for single and parallel flow double effect water-lithium bromide vapor absorption systems, *Int. J. Sci. Technol.* 2 (2012) 85-94.
- [28] N. Ezzine, B. Barhoumi, M. Mejbri, K. Chemkhi, S.A. Bellagi, Solar cooling with the absorption principle: first and second law analysis of an ammonia-water double-generator absorption chiller, desalination Strategies in South Mediterranean countries, *Desalination* 168 (2004) 137-144.
- [29] O.M. Ibrahim, S.A. Klein, Thermodynamic properties of ammonia water mixtures, *ASHRAE Trans.* 99 (1993) 1495-1502.
- [30] S. Libotean, D. Salavera, M. Vallès, X. Esteve, A. Coronas, Vapour-liquid equilibrium of ammonia þ lithium nitrate þ water and ammonia þ lithium nitrate solutions from (293.15 to 353.15) K, *J. Chem. Eng. Data* 52 (3) (2007) 1050- 1055.
- [31] S. Libotean, A. Martín, D. Salavera, M. Vallès, X. Esteve, A. Coronas, Densities, viscosities, and heat capacities of ammonia þ lithium nitrate and ammonia þ lithium nitrate þ water solutions between (293.15 and 353.15) K, *J. Chem. Eng. Data* 53 (10) (2008) 2383-2388.
- [32] Duffie JA, Beckman WA. *Solar engineering of thermal processes*. N.Y.: John Wiley and Sons; 1991.
- [33] H.Vettrivel and P.Mathiazhagan. Comparison Study of Solar Flat Plate Collector with Single and Double Glazing Systems. *International journal of renewable energy research*. Vol.7, No.1, 2017.